

Frequency glides in the impulse responses of auditory-nerve fibers

Laurel H. Carney,^{a)} Megean J. McDuffy, and Ilya Shekhter

Boston University Hearing Research Center and Department of Biomedical Engineering, Boston University, 44 Cummings Street, Boston, Massachusetts 02215

(Received 24 July 1998; revised 2 November 1998; accepted 15 January 1999)

Previous reports of frequency modulations, or glides, in the impulse responses of the auditory periphery have been limited to analyses of basilar-membrane measurements and responses of auditory-nerve (AN) fibers with best frequencies (BFs) greater than 1.7 kHz. These glides increased in frequency as a function of time. In this study, the instantaneous frequency as a function of time was measured for impulse responses of AN fibers in the cat with a range of BFs (250–4500 Hz). Impulse responses were estimated from responses to wideband noise using the reverse-correlation technique. The impulse responses had increasing frequency glides for fibers with BFs greater than 1500 Hz, nearly constant frequency as a function of time for BFs between 750 and 1500 Hz, and decreasing frequency glides for BFs below 750 Hz. Over the levels tested, the glides for fibers at all BFs were nearly independent of stimulus level, consistent with previous reports of impulse responses of the basilar membrane and AN fibers. Implications of the different glide directions observed for different BFs are discussed, specifically in relation to models for the auditory periphery as well as for the derivation of impulse responses for the human auditory periphery based on psychophysical measurements. © 1999 Acoustical Society of America. [S0001-4966(99)03204-X]

PACS numbers: 43.64.Bt, 43.64.Pg, 43.66.Ba [RDF]

INTRODUCTION

The properties of auditory nerve (AN) fibers can be characterized using their responses to impulses, or clicks, as well as to wideband noise. These properties have implications for our understanding of signal processing in the auditory periphery and of the neural cues provided by the periphery to the central nervous system. Responses of neurons to wideband noise stimuli have been studied for many years in an effort to characterize both linear and nonlinear response properties (e.g., deBoer, 1967; deBoer and deJongh, 1978; Marmarelis and Marmarelis, 1978; Eggermont *et al.*, 1983; Carney and Yin, 1988; Eggermont, 1993). The cross-correlation function of the response of the system to a wideband noise with the stimulus waveform provides an estimate for the system's first-order Wiener kernel (Lee and Schetzen, 1965). For a linear system, the first-order kernel is also the impulse response.

This cross-correlation analysis technique has been successfully applied to mechanical measurements of basilar-membrane motion (deBoer and Nuttall, 1997; Recio *et al.*, 1997). These measurements have characterized the impulse responses as narrow-band signals having a frequency modulation, or glide. For these mid- to high-frequency (>~1.7 kHz) fibers or places, the carrier frequency of the tuned impulse response increases as a function of time from a frequency lower than the best frequency (BF, the frequency to which the system is most responsive¹) up to the BF. The glides estimated from responses to wideband noise are consistent with impulse responses measured in the same co-

chleae using click stimuli (deBoer and Nuttall, 1997). The increasing frequency glides are also consistent with other reports of mechanical measurements of click responses from the base of the cochlea (Robles *et al.*, 1976; Recio *et al.*, 1998). deBoer and Nuttall (1997) referred to impulse responses based on click responses as *direct* impulse responses, and those estimated from noise responses as *indirect* impulse responses.

Characterization of the tuning of AN fibers based on responses to wideband noise requires an extension of the cross-correlation technique. Because the response of a fiber is a series of action potentials, rather than a continuous-time waveform, one cannot perform a simple cross correlation between the stimulus waveform and the response. However, a spike-triggered average of the stimulus waveform preceding each action potential yields a derived impulse response, the reverse-correlation (revcor) function (deBoer, 1967; deBoer and Kuyper, 1968; Møller, 1977; deBoer and deJongh, 1978; Marmarelis and Marmarelis, 1978; Eggermont *et al.*, 1983). Equivalently, a cross correlation between the noise stimulus waveform and the peri-stimulus time (PST) histogram constructed from responses to multiple repetitions of the stimulus yields an estimate of the impulse response (Møller, 1977).

The reverse-correlation procedure is only successful for relatively low-frequency AN fibers (BFs <~4000 Hz) because it requires phase-locking of the fiber to the fine structure of the stimulus waveform. Revcor functions for low-frequency AN fibers are consistent with click responses measured for the same fibers (Carney and Yin, 1988), indicating that this technique for the indirect estimate of the AN impulse response is consistent with direct estimates of impulse responses.

^{a)} Author to whom correspondence should be addressed. Electronic mail: carney@bu.edu

Pseudolinear characterizations of AN fibers across a range of stimulus levels provide a characterization of AN fibers that is adequate for predicting temporal response properties to resonant stimuli at different sound levels (Carney and Yin, 1988). A population of revcor functions has served as a basis for a pseudolinear model for a population of AN fibers (Carney and Yin, 1988) as well as for a nonlinear, time-varying model for AN responses to arbitrary stimuli (Carney, 1993). However, these models were based on simple parameterizations of the revcor functions as gammatone functions. The gammatone models used to characterize AN impulse responses have constant frequency as a function of time, and thus do not accurately represent impulse responses that contain frequency glides.

Reports of frequency glides in the revcor functions of AN fibers have been consistent with the descriptions of the direct and indirect impulse responses of the basilar membrane. Møller and Nilsson (1979; also Møller, 1981, 1983) illustrated an increasing frequency glide in the revcor functions for two rat AN fibers with BFs of approximately 2 and 3 kHz. deBoer and Nuttall (1997) reported increasing frequency glides in revcor functions for AN fibers with BFs as low as 3 kHz. They also reported increasing frequency glides in impulse responses derived from the phase measurements of tuning curves of AN fibers with BFs as low as 1.76 kHz (deBoer and Nuttall, 1997).

The goal of this study was to characterize the impulse responses of AN fibers with low to moderate BFs, ranging from approximately 250 to 4500 Hz. Across this frequency range, it is possible to measure indirect impulse responses using the reverse-correlation technique. Revcor functions of a large population of AN fibers (Carney and Yin, 1988; Carney, 1990) were examined in this study. The nature of the frequency glides in these derived impulse responses and the variation of the glides as a function of stimulus level were investigated. The frequency glides are consistent with descriptions of the shift in peak frequency of tuning as a function of stimulus level (deBoer and Nuttall, 1997; Recio *et al.*, 1997); that is, changes in the latency of the envelope of the impulse response as a function of level, along with the underlying (but level-independent) frequency glide, result in apparent shifts in the tuning as a function of level. For example, for BFs with glides that increase as a function of time, responses to high-level stimuli are determined by impulse responses that peak during the early, low-frequency portion of the frequency glide. Alternatively, responses to low-level stimuli are determined by impulse responses that peak at longer latencies, during the high-frequency part of the glide. Thus, the increasing frequency glides at high BFs are consistent with a downward shift in the peak frequency of tuning as stimulus level increases. Because some low-BF fibers have been described as having shifts in tuning that go in the opposite direction, it was not anticipated that the glides would necessarily be similar to those described for high-BF measurements. For example, very low-BF (<1000 Hz) fibers have been described as having peak frequencies that shift *upwards* as stimulus level increases (Evans, 1981), which is opposite in direction to the shift seen for high-BF fibers (Evans, 1981; Møller, 1977) and basilar-membrane

measurements made at high-BF places (Rhode, 1971; Sellick *et al.*, 1982; Robles *et al.*, 1986; deBoer and Nuttall, 1997; Recio *et al.*, 1997, 1998). The frequency modulations, or glides, in the impulse responses of AN fibers with BFs less than 1500 Hz reported in this study have different slopes than those previously reported for responses of fibers with higher BFs (Møller and Nilsson, 1979; Møller, 1981, 1983) or high-frequency places on the basilar membrane (deBoer and Nuttall, 1997; Recio *et al.*, 1997, 1998). Flat or decreasing frequency glides for fibers with BFs below 1500 Hz were observed in this study.

These frequency glides have interesting implications both for our understanding of signal processing in the auditory periphery and for cochlear models (Møller and Nilsson, 1979; deBoer and Nuttall, 1997; Recio *et al.*, 1998). The association of level-dependent shifts in peak frequency with the compressive nonlinearity make the time and level dependence of the frequency glides an important issue. As pointed out by deBoer and Nuttall (1997), the presence of the glide in both the indirect impulse response based on steady-state noise responses and in the actual impulse response indicates that it is not a reflection of a time-varying nonlinearity. In addition, they report that the glide is remarkably consistent over a wide range of stimulus levels, consistent with the reports of Recio *et al.* (1997, 1998). This was also the case for AN fibers in this study, regardless of the direction or slope of the glide. The frequency glide does not appear to be directly associated with the active process or the associated compressive nonlinearity; the frequency glide persists nearly unchanged across the wide range of levels tested (20–80 dB SPL), while the bandwidth and gain of the system vary.

Impulse responses with frequency glides have recently arisen in another area of auditory research: impulse responses with upward frequency glides (gammachirps) have been proposed to model the filters associated with asymmetrical psychophysical tuning curves (Iriño and Patterson, 1997). However, because the asymmetry of psychophysical tuning curves varies with stimulus level (e.g., Rosen and Baker, 1994), Iriño and Patterson (1997) proposed that the peripheral filters should have glides that vary in slope as a function of stimulus level. Such filters would be at odds with measurements of both direct and indirect impulse responses from the auditory periphery. The variations in asymmetry of psychophysical tuning curves as a function of level must arise from properties other than changes in the slope of frequency glides in the impulse responses.

I. METHODS

Noise responses of AN fibers were obtained from a data archive collected as part of previous studies (Carney and Yin, 1988; Carney, 1990). The physiological procedures used to obtain the functions are detailed in those papers. Briefly, the responses of AN fibers to wideband (10-kHz bandwidth) noises were recorded in barbiturate-anesthetized cats. Typically, 40 repetitions at each sound level of an 800-ms duration noise sample were obtained at 1-s intervals. Sound levels reported here are in dB SPL (computed over the 10-kHz bandwidth of the noise) for consistency with

other studies, rather than the peak-equivalent levels reported previously (Carney and Yin, 1988; Carney, 1990).

The results presented were based on revcor functions, typically computed for noise responses measured at two or more sound levels, for 214 fibers from 13 cats. The original (unsmoothed) revcor functions are accessible for further study via an ftp site (Appendix A).

Each revcor function was computed using the cross-correlation function for the stimulus waveform and the PST histogram of the noise response (deBoer and deJongh, 1978). PST histograms were binned at 50- μ s resolution, which matched the sampling time of the stimulus waveform. A one-octave bandpass filter, centered at the peak frequency of the spectrum of the revcor function, was used to smooth the revcor functions. The 8th-order bandpass filter was implemented in MATLABTM, and the output signal was compensated for the delay of the filter. The filtered revcor functions were tested to ascertain that the filter did not introduce any phase distortion that could have affected the positions of zero crossings; this test was accomplished by superimposing the filtered and original signals and carefully comparing the locations of the zero crossings.

At very low stimulus levels, the BF of the revcor function matches the characteristic frequency (CF) based on a threshold-tuning curve; however, as stimulus level increases, these two frequencies may diverge, depending on CF (e.g., Evans, 1981). The BF was estimated using the peak frequency of the spectrum of the revcor function, computed with the fast Fourier transform. When glides were studied across several SPLs, the average BF across the SPLs was used as the fiber's BF [Fig. 7(A)].

The instantaneous frequency of the revcor functions was estimated in two ways: using a Hilbert-transform technique and using zero crossings. Using Hilbert-transform techniques, the instantaneous frequency (IF) and envelope of an analytic signal could be determined (Appendix B). This technique was used to analyze the impulse responses derived from basilar-membrane responses to noise (deBoer and Nuttall, 1997; Recio *et al.*, 1997). A preliminary study found that this technique was also appropriate for AN revcor functions (Shekhter, 1997; Shekhter and Carney, 1997).

A limitation of the Hilbert-transform technique is noise; because the derivative of the phase of the analytical signal is involved in the computation of the IF, the technique is very sensitive to noise in the original signal. In addition, large fluctuations obscure the estimate of IF derived from the Hilbert transform when the amplitude of the envelope of the signal decreases (deBoer and Nuttall, 1997). An alternative technique for estimating instantaneous frequency is to compute the intervals between zero crossings of the signal (Møller, 1977). This technique typically results in a less noisy estimate of IF, but provides fewer measures of IF as a function of time. The two methods provide results that are generally consistent with each other, as shown below (Fig. 2). The zero crossings provided a simple description of the major trends in the IF as a function of time that was less prone to fluctuations caused by either noise in the signal or changes in the envelope amplitude.

The IF estimated using the intervals between zero cross-

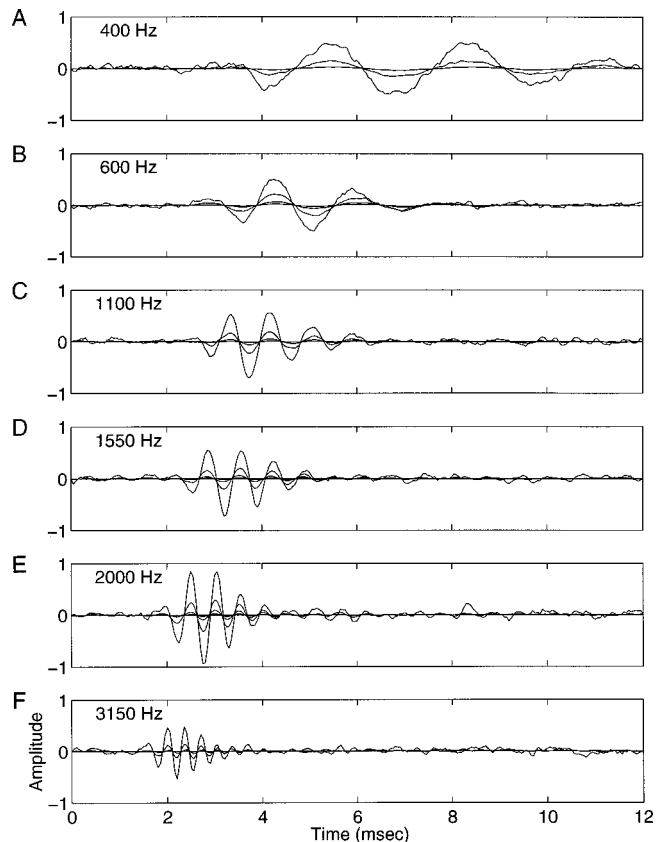


FIG. 1. Revcor functions for six fibers. Revcors for several SPLs are overlaid in each panel, with the higher amplitude waveforms corresponding to the higher SPLs. The BF computed from the revcor function at the lowest SPL is indicated in each panel. Amplitudes are in arbitrary units; all waveforms were normalized by the same value here and in all subsequent figures. These waveforms illustrate the revcor functions after a simple 3-pt smooth was applied; the octave-band filter used in subsequent analysis was not applied to the waveforms shown here. (A) Unit 86204u3; 60, 70, 80 dB SPL. (B) Unit 86100u8; 50, 60, 70, 80 dB SPL. (C) Unit 86100u24; 50, 60, 70, 80 dB SPL. (D) Unit 86065u5; 20, 30, 40, 50, 60, 70, 80 dB SPL. (E) Unit 86100u25; 30, 40, 50, 60, 70, 80 dB SPL. (F) Unit 86204u28; 50, 60, 70, 80 dB SPL. The same waveforms were used for the analyses of instantaneous frequency illustrated in Fig. 3, with different symbols for each SPL.

ings was susceptible to dc bias introduced in the waveform before determination of zero crossings, or indeed, to alterations of the dc content of the signal that were introduced by smoothing techniques. In order to minimize the contribution of dc fluctuations (which are unavoidable over short-time intervals of amplitude-modulated signals), the following procedure was used: The time range to be analyzed was determined by computing the envelope of the revcor function (Appendix B) and finding the time range for which the amplitude of the envelope was within 12 dB of the peak of the envelope (deBoer and Nuttall, 1997). The mean (dc) value was then computed over an integer number of cycles of the best frequency centered within this time range. This mean value was then subtracted from the waveform before zero crossings were detected. Zero crossings were determined by identifying the two time samples in the 50- μ s resolution waveform that spanned the crossing, and then applying linear interpolation between the two time samples.

A related technique for computing IF is to measure the distances between maxima and/or minima in the impulse re-

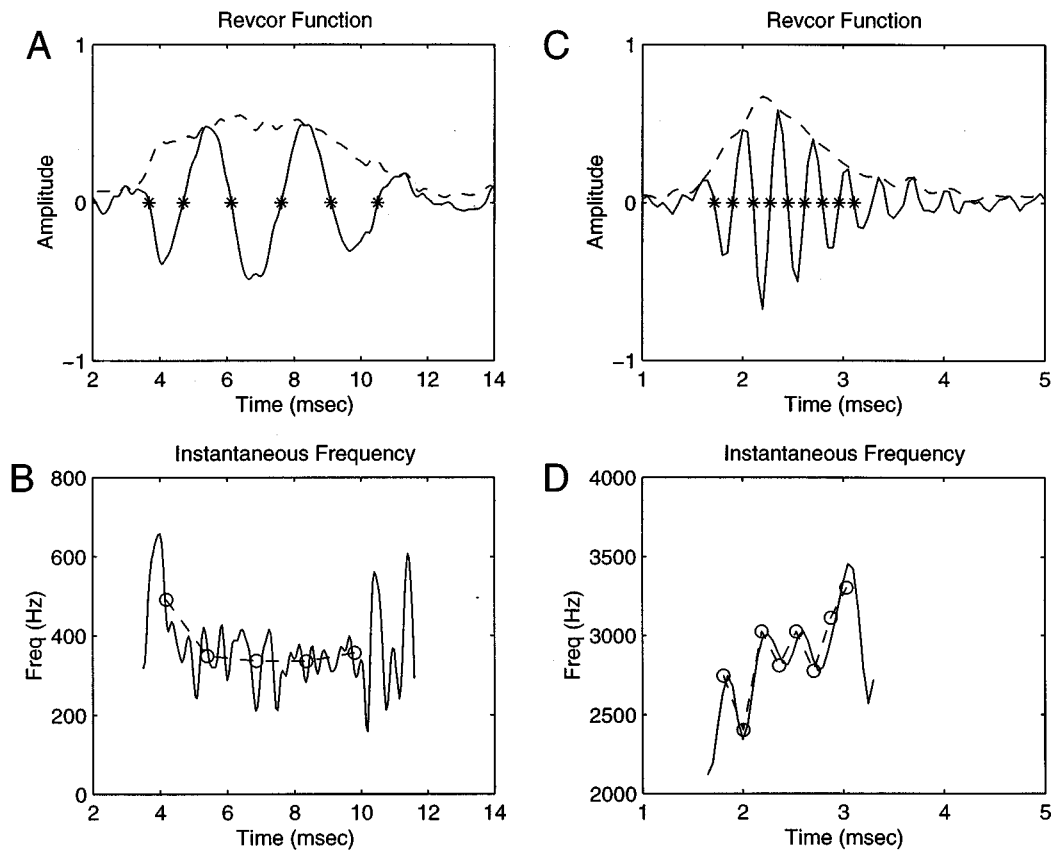


FIG. 2. (A) Revcor function for an AN fiber with BF=400 Hz [same as in Fig. 1(A)]. The dashed line is the envelope computed with the Hilbert transform (Appendix B). A 3-point smooth was applied to the envelopes to reduce the influence of high-frequency noise on the determination of the temporal window to be analyzed (see methods). Asterisks indicate zero crossings. (B) Same as (A), for an AN fiber with BF=3150 Hz [same fiber as in Fig. 1(F)]. (C), (D) IF for each fiber computed using the Hilbert transform (solid lines) and using zero crossings (circles connected by dashed line). Circles are positioned along the time axis midway through each zero-crossing interval.

sponse. This approach is not susceptible to changes in dc bias of the waveform; however, it is susceptible to high-frequency noise in the vicinity of the maxima and minima. Results using the latter approach were consistent with the dc-compensated zero-crossing approach for the majority of the fibers; however, the IFs based on maxima and minima were particularly noisy for the very low-BF fibers; thus, this approach was not used for the results presented here.

II. RESULTS

Revcor functions for six fibers with a range of BFs are illustrated in Fig. 1. Each panel shows revcor functions for a single fiber computed from noise responses at several SPLs; waveforms with higher amplitude peaks correspond to responses to higher amplitude stimuli. The amplitude of the revcor functions² (expressed in arbitrary units) in this figure, and all other figures, was normalized by the same value to allow comparison across plots. The fibers illustrated here were arbitrarily chosen from fibers that were studied at a number of SPLs; the properties of these responses were typical for the revcor functions in this study.

Changes in the distances between zero crossings can be observed directly in some of these plots. For the lowest BF fiber [Fig. 1(A)], the first two zero crossings were clearly more closely spaced than subsequent ones. Changes in the

zero crossings as a function of time were much smaller for the intermediate BF fibers. For the highest BF fiber [Fig. 1(F)], the zero crossings became more closely spaced as a function of time. Close scrutiny of previously reported revcor functions (e.g., Evans, 1985) and click responses (Kiang *et al.*, 1965) for fibers with different BFs also reveal changes over time in the intervals between zero crossings or intervals between histogram peaks that are similar to those shown in Fig. 1.

A striking feature of the revcor functions shown in Fig. 1 is that the zero crossings were nearly unchanged over a wide range of SPLs. This fact is consistent with earlier reports of AN revcors at several SPLs (Carney and Yin, 1988) and with click responses measured either in the AN (Kiang *et al.*, 1965) or basilar membrane (Recio *et al.*, 1998). The consistency of the zero crossings over a wide range of SPLs indicates that the instantaneous frequency, whether it changed or remained stationary over time, would be similar across SPLs.

The analysis of instantaneous frequency (IF) is illustrated in Fig. 2. Panels A and C show the revcor functions for two fibers at 80 dB SPL [same fibers as in Fig. 1(A),(F)]. The envelope of the revcor function, as determined by the Hilbert transform (Appendix B) is shown as the dashed line, and zero crossings are indicated by asterisks [Fig. 2(A),(C)]. The IF computed using the Hilbert transform is indicated as

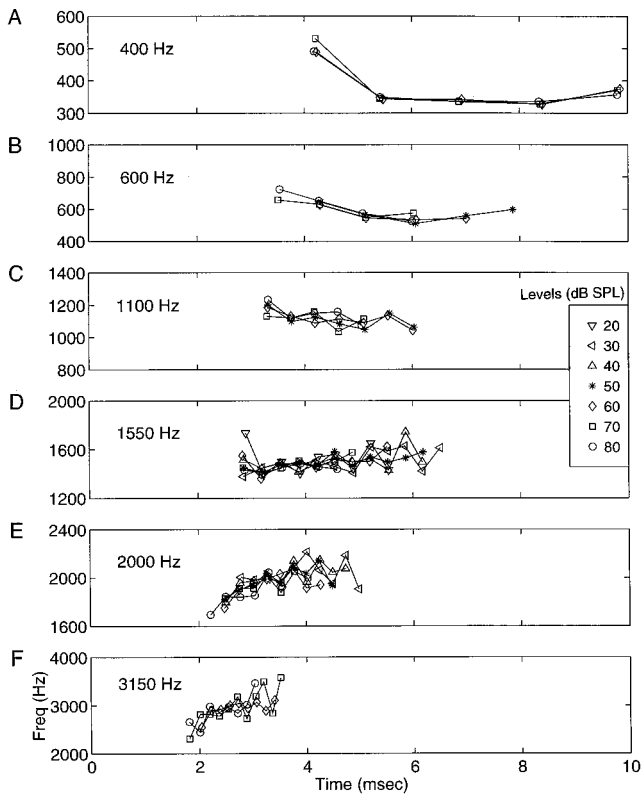


FIG. 3. IF trajectories as a function of time for the six fibers in Fig. 1, at several SPLs. Symbols for SPLs in the legend apply to all plots. IF was computed from zero crossings, as illustrated in Fig. 2. The BF of each fiber, computed from the revcor function at the lowest SPL, is indicated on each plot.

the solid line [Fig. 2(B),(D)]. These functions tended to be noisy, as described in the methods, and they were particularly sensitive to noise when the amplitude of the envelope dropped to low values (at the beginning and end of each waveform). The IF computed on the basis of zero crossings is illustrated by the circles and dashed lines. The IF com-

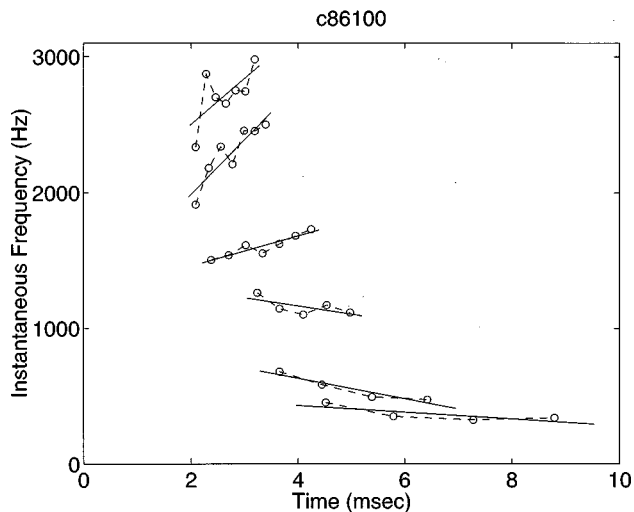


FIG. 4. IF trajectories at 80 dB SPL for six fibers from one cat. IFs were determined using zero crossings (circles connected by dashed lines). Solid lines are 1st-order regressions fit through each trajectory. Units 2, 7, 18, 20, 22, and 26 from cat 86100.

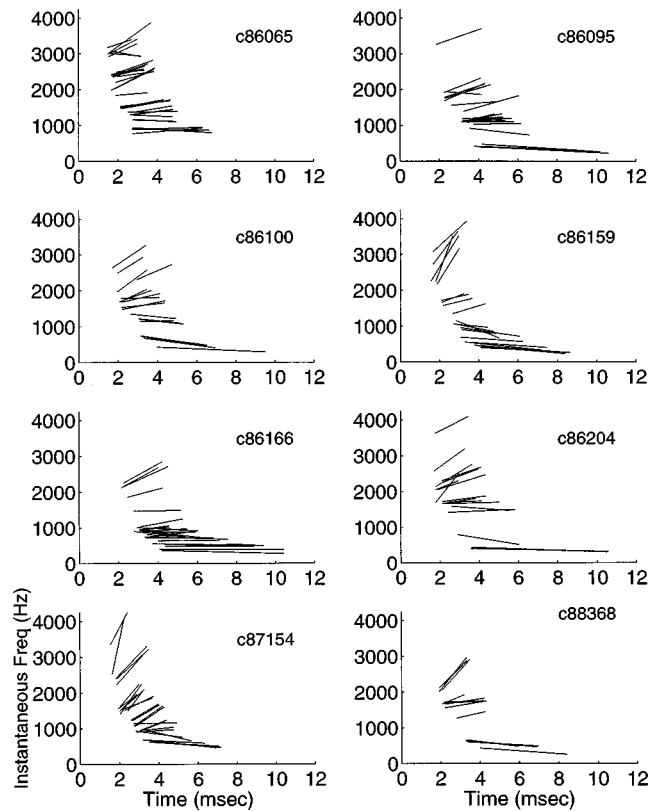


FIG. 5. 1st-order regression lines through IF trajectories for groups of fibers from eight cats. All fibers studied in each cat are included in each plot. IF trajectories were based on zero crossings. All responses were at 80 dB SPL.

puted from zero crossings was quite consistent with the IF from the Hilbert transform [Fig. 2(D)], including some of the fluctuations over time that were characteristic of especially higher-BF results from the basilar membrane (see deBoer and Nuttall, 1997).

Figure 3 illustrates the IFs for the six fibers in Fig. 1, each computed at several SPLs using zero crossings. The lowest BF fiber [Fig. 3(A)] had an IF that decreased as a function of time, whereas the highest BF fiber [Fig. 3(F)] had an increasing frequency glide. Intermediate BFs had smaller changes in IF as a function of time, progressing gradually from negative slopes at very low BFs to positive slopes at higher BFs. Consistent with the nearly invariant zero crossings at different SPLs (Fig. 1), the IF trajectories for each fiber (Fig. 3) were very similar over the range of SPLs studied here.

Figure 4 illustrates IF trajectories based on zero crossings for several fibers from one cat at one SPL (80 dB SPL). Each trajectory was fit by a first-order linear regression. These regressions and their slopes will be reported in the following figures. For nearly all fibers studied, a 1st-order regression provided a reasonable representation of the IF glide. Some fibers had glides that were not linear functions of time; for example, several (but not all) of the very low-BF fibers had a bend in the IF trajectory [see the two lowest BF fibers in Fig. 4 and the fiber in Fig. 2(B) and Fig. 3(A)]. However, higher-order regressions did not improve the characterization of the major trends in the glides across the population of fibers studied. Furthermore, there was no improve-

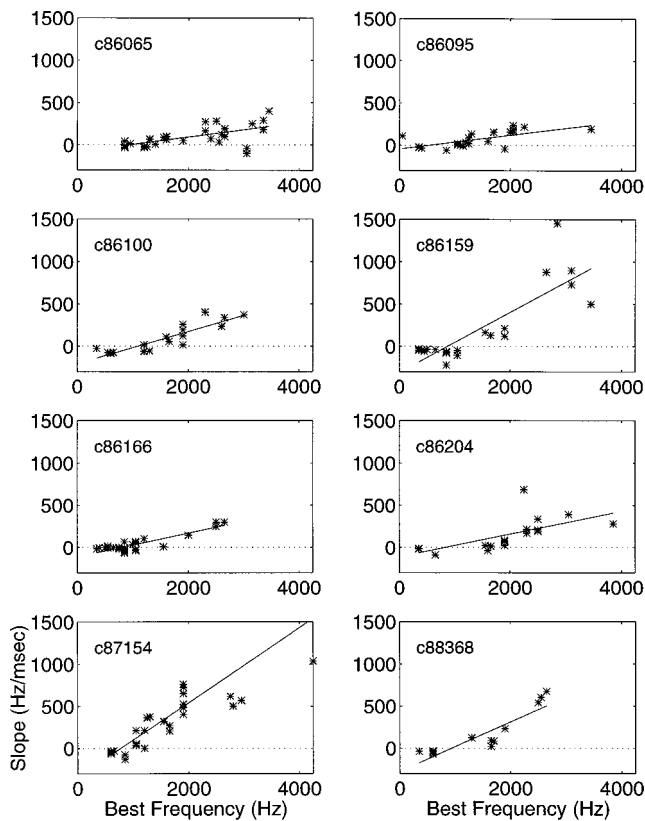


FIG. 6. Slopes of the trajectories in Fig. 5 as a function of best frequency (BF). BF was estimated by the peak of the fast Fourier transform of the revcor function. Each asterisk indicates the slope of a single regression line in Fig. 5. The solid lines are first-order regressions for each set of data points.

ment in characterizing these glides by representing them as functions of $\log(t)$, which was the form of the gammachirp suggested by Irino and Patterson (1997). Functions of this type could not provide a simple representation for IF glides across the range of BFs, because the glides vary significantly across BF in direction and overall latency.

Figure 5 illustrates the same characterization as in Fig. 4 for the eight cats in which several fibers across a range of BFs were studied. All responses shown in this figure are for 80-dB SPL noise stimuli. Only the 1st-order regression lines are shown to reduce the complexity of the figure. The major trend in the data is apparent in all cats: positively sloping IF glides at high BFs, flat trajectories at BFs near 1000 Hz, and negatively sloping IF glides at very low BFs.

Figure 6 shows slopes of the trajectories in Fig. 5 as a function of best frequency (BF). Each asterisk indicates the slope of a single regression line in Fig. 5. The slope of the IF trajectories (in Hz/ms) increased as a function of BF in all cats. Slopes were typically positive and relatively large for high BFs, small for BFs near 1000 Hz, and negative for very low BFs.

Trends in the slope of the IF as a function of BF are also apparent in Fig. 7, which illustrates the slopes for 214 fibers from all 13 cats. For the results shown in this figure, the IF was estimated at all SPLs for each fiber. Responses to SPLs that yielded a clean IF (e.g., more than three zero crossings and at SPLs high enough to yield detectable revcor functions) were included in this population plot. IFs for all SPLs

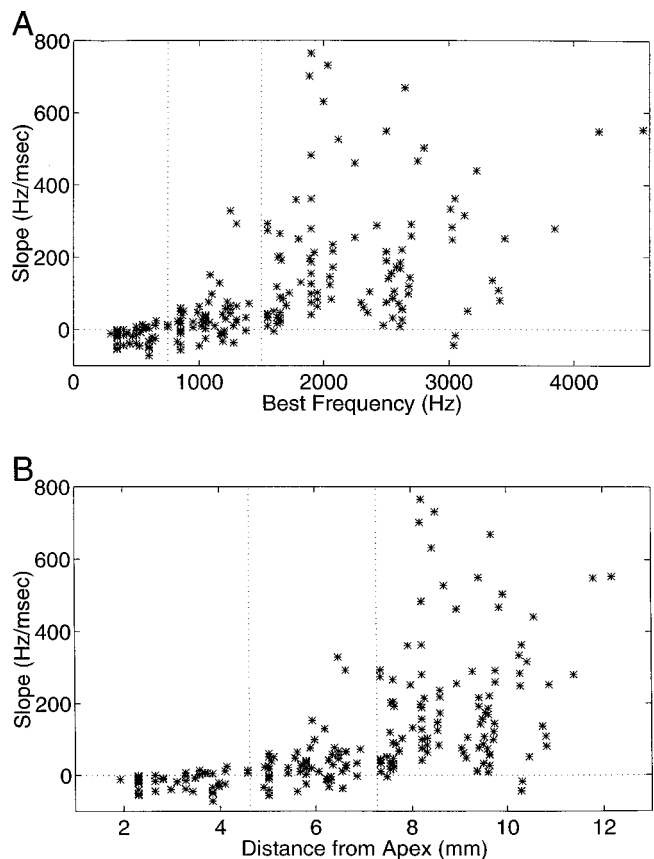


FIG. 7. Slope of the 1st-order regressions of IF trajectories based on responses at all SPLs studied for 214 fibers in 13 cats. The BF for each fiber was determined by averaging the BFs across the SPLs studied. (A) Results plotted on a linear frequency axis. (B) Results plotted on a place axis, using Liberman's (1982) expression for place as a function of CF. Vertical dotted lines are positioned by eye at 750 and 1500 Hz to illustrate trends over different frequency regions.

were used to determine the 1st-order regression lines; the average BF across the SPLs studied for each fiber was used to determine the position along the BF axis.

Figure 7(A) illustrates the slope of the 1st-order regression for each fiber, plotted in terms of linear frequency. Figure 7(B) plots the slope of the IF regression as a function of distance along the basilar membrane, using Liberman's (1982) function for the relationship between CF and place along the cochlea. The latter plot illustrates the spatial range along the basilar membrane in the cat for which the IF trajectories are negative or relatively flat. Based on previous reports of increasing glides for high-BF fibers and basilar-membrane (BM) responses, it would be assumed that the IF trajectories remain positive for all basilar-membrane positions further from the apex (i.e., BFs higher than 4 kHz).

The vertical dotted lines in each plot (Fig. 7) were positioned at 750 and 1500 Hz to demarcate the three interesting regions of BFs and IF slopes. For fibers with BFs below 750 Hz, 78% of the slopes of the IF trajectories were negative (38 out of 49 fibers), and the positive slopes were quite small (all below 25 Hz/ms). For fibers with BFs between 750 and 1500 Hz, 70% of the IF trajectories had positive slopes (43 out of 61 fibers). Again, these slopes were relatively small: 93% had slopes less than 100 Hz/ms. Above 1500 Hz, the IF trajectories of nearly all (97%, 101 out of 104) fibers

had positive slopes. The size of the slopes varied a great deal for the high-BF fibers; some of this variability was due to combining responses across cats. The results in Fig. 5 for individual cats showed less variability within each animal; Fig. 5 also showed large differences in the absolute values of the high-BF slopes across animals.

III. DISCUSSION

These results show that the frequency modulations, or glides, in the impulse responses of low-frequency AN fibers (< 1500 Hz) are inherently different from those at high BFs. Whereas the high-BF AN and basilar-membrane responses reported previously all had glides that increased in frequency as a function of time, the direction of the glides is the opposite at very low frequencies. Furthermore, in the mid-frequency region (750–1500 Hz), the glides are relatively flat.

The available database did not include responses to very high SPL stimuli, so it cannot be determined whether the glides would remain unchanged at very high SPLs. Recently, Lin and Guinan (1998) reported significant changes in the impulse responses of AN fibers in the cat in response to very high-level clicks, consistent with a change in the nature of the mechanical input to the hair cells at very high levels. More work is required to determine whether similar changes would be found in indirect estimates of impulse responses based on noise responses.

As pointed out for measurements of high-BF AN fibers and places (deBoer and Nuttall, 1997; Recio *et al.*, 1997, 1998), the trajectories of IF do not change significantly with SPL over the levels studied here. This result is interesting for many reasons. First, it indicates that the glides are not a property due to nonlinearities of the inner ear, such as the active process, which varies the gain and bandwidth of tuning as a function of SPL over the range of levels studied here. Second, impulse responses that have nearly unchanged zero crossings as a function of level, for which there is now an abundance of evidence in both basilar-membrane and AN data, are not consistent with most existing models for cochlear mechanics (deBoer and Nuttall, 1997). Whereas phenomenological models, based on linear filters with carefully placed poles, can exhibit glides (deBoer and Nuttall, 1996, 1997; Shekhter and Carney, 1997), the challenge is to understand a nonlinear system with gain and bandwidth that change with SPL, but with IF trajectories that remain unchanged. A framework for considering the input–output cross-correlation functions for nonlinear systems, and for relating them to linear systems with equivalent cross-correlation functions, has recently been outlined in deBoer's EQ-NL theory (deBoer, 1997). Thus, according to that theory, the results presented here suggest that there must also be a related class of linear systems (as well as nonlinear) that exhibit the nearly invariant IF over a wide range of SPLs, while varying in other respects (e.g., gain and bandwidth).

The constraints that the increasing IF glides for mid- to high BFs have placed on cochlear models have been recognized previously (Møller and Nilsson, 1979; deBoer and Nuttall, 1997). The additional evidence that the slope and direction of the glides changes as a function of BF places

new constraints on these models. An increasing frequency glide is not an inherent property of the impulse responses of AN fibers across all BFs. Either the properties of the cochlear mechanics that contribute to the glide must vary along the length of the cochlea, or interactions at the low-frequency end of the cochlea, within approximately 6 or 7 mm of the helicotrema [Fig. 7(B)], must result in significant changes in the nature of the IF glides.

Increasing frequency glides have also been hypothesized to be a property of impulse responses for tuning in the human auditory periphery based on psychophysical tuning curves (Iriño and Patterson, 1997). The asymmetry of psychophysical tuning curves was modeled by a filter that has a frequency-modulated impulse response, the gammachirp. However, proposed changes in the slope of the gammachirp's IF glide as a function of SPL, which would produce the desired changes in the asymmetry of the filters as a function of SPL, would be inconsistent with this and other reports that the IF glides of the auditory periphery are nearly unchanged as a function of SPL.

Future work will explore the implications for human perception of the IF glides, including their change as a function of BF. The influence of the IF trajectory of the impulse response on the responses to simple and complex sounds will be complicated. The trajectories in IF seen in the impulse response would be hypothesized to influence both the rate and temporal response properties of individual AN fibers, as well as the spatiotemporal response patterns across the population of AN fibers.

ACKNOWLEDGMENTS

This study was based on data collected during research supported by grant NINCDS-NS12732 while working at the University of Wisconsin with Professor Tom Yin. We acknowledge the generous assistance of Dr. Yin and Ravi Kochhar in obtaining the data files and copies of the data notebooks, which had been carefully maintained over the years. At Boston University, this work has been supported by NSF-IBN9601215. We acknowledge the many helpful comments and discussions of this work with our colleagues Egbert deBoer, David Cameron, Michael Heinz, Tai Lin, Christine Mason, Susan Moscynski, and Ling Zheng.

APPENDIX A: INSTRUCTIONS FOR ACCESSING REVCOR FUNCTIONS VIA FTP

The unsmoothed revcor functions for all the fibers included in this study are available via ftp at the address: *engc.bu.edu* Login as *anonymous*, with your user name as the password. Type *cd/pub/andata* to move to the proper directory. Further instructions about the file formats and file names are in the *readme.txt* file in this directory.

APPENDIX B: TIME-DOMAIN ANALYSIS OF REVCOR FUNCTIONS USING THE HILBERT TRANSFORM

A revcor function $h(t)$ can be decomposed into its envelope and instantaneous frequency using the Hilbert transform (e.g., Haykin, 1994). First, an analytic signal is formed

$$a(t) = h(t) + j\hat{h}(t),$$

where $\hat{h}(t)$ is the Hilbert transform of $h(t)$, and $j = \sqrt{-1}$. Then, the envelope of the revcor function $\text{env}(t)$ is equal to the magnitude of the complex function $a(t)$

$$\text{env}(t) = |a(t)|,$$

while the instantaneous frequency (IF, in Hz) is proportional to the derivative of the phase angle of $a(t)$

$$\text{IF}(t) = [d/dt\{\angle a(t)\}]/(2\pi).$$

¹In this manuscript, the term best frequency (BF) will be used to describe the center frequency of tuning of AN fibers and places along the basilar membrane. BF is most often used to describe tuning based on suprathreshold stimuli, whereas characteristic frequency (CF) is generally used to describe tuning for threshold level stimuli. At low stimulus levels, estimates of BF based on revcor functions are approximately equal to CF (deBoer, 1973). Here, for simplicity, the term BF will be used throughout, because the measures presented here are all based on suprathreshold stimuli.

²The amplitude of a revcor function is influenced by the number of action potentials, the degree of phase-locking to energy near BF within the noise stimulus, and the amplitude and units of the stimulus waveform used in the analysis (e.g., the waveform may be expressed in volts or Pa).

Boer, E. de (1967). "Correlation studies applied to the frequency resolution of the cochlea," *J. Aud. Res.* **7**, 209–217.

Boer, E. de (1973). "On the principle of specific coding," *J. Dyn. Syst., Meas., Control* **95G**, 265–273.

Boer, E. de (1997). "Connecting frequency selectivity and nonlinearity for models of the cochlea," *Aud. Neurosci.* **3**, 377–388.

Boer, E. de, and Jongh, H. R. de (1978). "On cochlear encoding: Potentialities and limitations of the reverse correlation technique," *J. Acoust. Soc. Am.* **63**, 115–135.

Boer, E. de, and Kuyper, P. (1968). "Triggered correlation," *IEEE Trans. Biomed. Eng.* **15**, 169–179.

Boer, E. de, and Nuttall, A. L. (1996). "Cochlear travel time and minimum phase," *Assoc. Res. Otolaryngol.* **19**, 57.

Boer, E. de, and Nuttall, A. L. (1997). "The mechanical waveform of the basilar membrane. I. Frequency modulations ("glides") in impulse responses and cross-correlation functions," *J. Acoust. Soc. Am.* **101**, 3583–3592.

Carney, L. H., and Yin, T. C. T. (1988). "Temporal coding of resonances by low-frequency auditory nerve fibers: Single fiber responses and a population model," *J. Neurophysiol.* **60**, 1653–1677.

Carney, L. H. (1990). "Sensitivities of cells in the anteroventral cochlear nucleus of cat to spatio-temporal discharge patterns across primary afferents," *J. Neurophysiol.* **64**, 437–456.

Carney, L. H. (1993). "A model for the responses of low-frequency auditory nerve fibers in cat," *J. Acoust. Soc. Am.* **93**, 401–417.

Eggermont, J. J. (1993). "Wiener and Volterra analyses applied to the auditory system," *Hearing Res.* **66**, 177–201.

Eggermont, J. J., Johannesma, P. I. M., and Aertsen, A. M. H. (1983). "Reverse-correlation methods in auditory research," *Q. Rev. Biophys.* **16**, 341–414.

Evans, E. F. (1981). "The dynamic range problem: Place and time coding at the level of cochlear nerve and nucleus," in *Neuronal Mechanisms of*

Hearing, edited by J. Syka and L. Aitkin (Plenum, New York), pp. 69–86.

Evans, E. F. (1985). "Aspects of the neural coding of time in the mammalian peripheral auditory system relevant to temporal resolution," in: *Time Resolution in Auditory Systems*, 11th Danavox Symposium, edited by A. Michelsen (Springer, New York), pp. 74–95.

Haykin, S. S. (1994). *Communication Systems* (Wiley, New York).

Irino, T., and Patterson, R. D. (1997). "A time-domain, level-dependent auditory filter: The gammachirp," *J. Acoust. Soc. Am.* **101**, 412–419.

Kiang, N. Y.-S., Watanabe, T., Thomas, E. C., and Clark, L. F. (1965). "Discharge patterns of single fibers in the cat's auditory nerve," MIT Research Monograph No. 35 (MIT, Cambridge, MA).

Lee, Y. W., and Schetzen, M. (1965). "Measurement of the Wiener kernels of a non-linear system by cross-correlation," *Int. J. Control* **2**, 237–254.

Lieberman, M. C. (1982). "The cochlear frequency map for the cat: labelling auditory nerve fibers of known characteristic frequency," *J. Acoust. Soc. Am.* **72**, 1441–1449.

Lin, T., and Guinan, Jr., J. J. (1998). "Auditory-nerve discharge patterns in response to high-sound-level clicks suggest that two different resonances are involved," *Assoc. Res. Otolaryngol.* **21**, 137.

Marmarelis, P. Z., and Marmarelis, V. Z. (1978). *Analysis of Physiological Systems: the White Noise Approach* (Plenum, New York).

Möller, A. R. (1977). "Frequency selectivity of single auditory-nerve fibers in response to broadband noise stimuli," *J. Acoust. Soc. Am.* **62**, 135–142.

Möller, A. R. (1981). "Coding of complex sounds in the auditory nervous system," in *Neuronal Mechanisms of Hearing*, edited by J. Syka and L. Aitkin (Plenum, New York), pp. 87–103.

Möller, A. R. (1983). *Auditory Physiology* (Academic, New York), pp. 220ff and Fig. 3.13.

Möller, A. R., and Nilsson, H. G. (1979). "Inner ear impulse response and basilar membrane modelling," *Acustica* **41**, 258–262.

Recio, A., Narayan, S. S., and Ruggero, M. A. (1997). "Wiener-kernel analysis of basilar-membrane responses to white noise," in *Diversity in Auditory Mechanics*, edited by E. R. Lewis, G. R. Long, R. F. Lyon, P. M. Narins, C. R. Steele, and E. Hecht-Poinar (World Scientific, Singapore), pp. 325–331.

Recio, A., Rich, N. C., Narayan, S. S., and Ruggero, M. A. (1998). "Basilar-membrane responses to clicks at the base of the chinchilla cochlea," *J. Acoust. Soc. Am.* **103**, 1972–1989.

Rhode, W. S. (1971). "Observations of the vibrations of the basilar membrane in squirrel monkeys using the Mössbauer technique," *J. Acoust. Soc. Am.* **49**, 1218–1231.

Robles, L., Rhodes, W. S., and Geisler, C. D. (1976). "Transient response of the basilar membrane measured in squirrel monkeys using the Mössbauer effect," *J. Acoust. Soc. Am.* **59**, 926–939.

Robles, L., Ruggero, M. A., and Rich, N. C. (1986). "Basilar membrane mechanics at the base of the chinchilla cochlea. I. Input–output functions, tuning curves and response," *J. Acoust. Soc. Am.* **80**, 1364–1374.

Rosen, S., and Baker, R. J. (1994). "Characterizing auditory filter nonlinearity," *Hearing Res.* **73**, 231–243.

Sellick, P. M., Patuzzi, R., and Johnstone, B. M. (1982). "Measurement of basilar membrane motion in the guinea pig using the Mössbauer technique," *J. Acoust. Soc. Am.* **72**, 131–141.

Shekhter, I. (1997). "A phenomenological model for nonlinear response properties of auditory-nerve fibers," Masters thesis, Boston University.

Shekhter, I., and Carney, L. H. (1997). "A nonlinear auditory nerve model for CF-dependent shifts in tuning with sound level," *Assoc. Res. Otolaryngol.* **20**, 617.